



Cluster-splitting bifurcation in a system of coupled maps

O. Popovych^{a,b}, A. Pikovsky^{a,*}, Yu. Maistrenko^b

^a Department of Physics, University of Potsdam, Am Neuen Palais, PF 601553, D-14415, Potsdam, Germany

^b Institute of Mathematics, National Academy of Sciences of Ukraine, 01601 Kyiv, Ukraine

Abstract

We consider cluster-splitting bifurcations in a system of globally coupled maps as coupling parameter decreases. At these transitions the number of clusters, i.e., groups of elements with identical dynamics, increases. We demonstrate that different cascades of cluster-splitting can occur, depending on statistics of redistribution of the oscillators between new-born clusters. © 2002 Elsevier Science B.V. All rights reserved.

Keywords: Coupled maps; Clustering; Bifurcation; Cluster splitting

1. Introduction

Ensembles of coupled chaotic oscillators have received a large attention in the last decade. Two typical models are usually studied in this context: lattices with local in space interaction [1,2], and populations with global (all-to-all) coupling [3–5]. The interesting phenomenon of non-trivial collective dynamics in such systems is a subject of intensive study using their transfer (Frobenius–Perron) operator [6], finite-size collective Lyapunov exponents [7,8], directed percolation universality class [9], and a linear response function [10]. Recently, an experimental investigation of 64 globally coupled chaotic electrochemical oscillators has been performed [11]. These studies have revealed, that already coupling of identical chaotic oscillators demonstrates non-trivial synchronization patterns.

Many aspects of the dynamics can be obtained already in the simplest model of globally coupled maps, introduced by Kaneko [12]

$$x_i(n+1) = (1 - \varepsilon)f(x_i(n)) + \frac{\varepsilon}{N} \sum_{j=1}^N f(x_j(n)), \quad i = 1, 2, \dots, N, \quad (1)$$

where $\mathbf{x} = \{x_i(n)\}_{i=1}^N$ is a state vector at time $n = 0, 1, \dots$, $\varepsilon \in \mathbb{R}$ is the coupling parameter, and $f : \mathbb{R} \rightarrow \mathbb{R}$ is a one-dimensional map. For further studies of this model, see, e.g., Refs. [13–20] and references therein.

An interesting form of asymptotic behavior that can arise in the system of globally coupled map (1) is clustering [12] or partial synchronization [21]. The population of oscillators splits into K subgroups

* Corresponding author.

E-mail address: pikovsky@stat.physik.uni-potsdam.de (A. Pikovsky).

$$\begin{aligned}
x_{i_1} = x_{i_2} = \dots = x_{i_{N_1}} &\stackrel{\text{def}}{=} y_1, & x_{i_{N_1+1}} = x_{i_{N_1+2}} = \dots = x_{i_{N_1+N_2}} &\stackrel{\text{def}}{=} y_2, & \dots, \\
x_{i_{N_1+N_2+\dots+N_{K-1}+1}} &= x_{i_{N_1+N_2+\dots+N_{K-1}+2}} = \dots = x_{i_N} &\stackrel{\text{def}}{=} y_K
\end{aligned} \tag{2}$$

called *clusters* such that all oscillators within a given cluster asymptotically move in synchrony. The number of variables x_i that synchronize into a given state y_j is denoted by N_j , such that $\sum_{j=1}^K N_j = N$. Note that, under the conditions above, system (1) can possess many different K -cluster states with the same variable distribution among the clusters [13]. Clustering has been also observed in experiments with chaotic [11] and periodic [22–24] dynamics.

In-cluster dynamics of a K -cluster state is governed by the K -dimensional system F_K of the form

$$y_i(n+1) = (1-\varepsilon)f(y_i(n)) + \varepsilon \sum_{j=1}^K p_j^{(K)} f(y_j(n)), \quad i = 1, \dots, K, \tag{3}$$

obtained after direct reduction of (1) to the cluster subspace Π_K defined by (2). This system is again a population of globally coupled maps, but the coupling comes with weight parameters $p_j^{(K)} = N_j/N$ corresponding to the relative number of variables x_i belonging to the j th cluster. One-cluster (or coherent) state, for instance, is characterized by the dynamics, where all elements in the ensemble considered display the same temporal variation. In this case, the dynamics is restricted to the diagonal $D_N = \{(x_1, x_2, \dots, x_N) | x_1 = x_2 = \dots = x_N\}$ and is governed by the one-dimensional map f .

Typically, with the decrease of the coupling parameter ε one observes an increase of the number of clusters. Indeed, in the limiting case of strongest coupling $\varepsilon = 1$ the one-cluster state is superstable: It appears in one time step. From the other side, for vanishing coupling, when dynamics of the mapping f is chaotic, no clusters appear. The whole phase diagram is rather complex (cf. [12]). In this paper, we focus on a certain aspect of the order–disorder transition in system (1), namely on the cluster-splitting bifurcations, at which the number of clusters increases. Moreover, we restrict mainly our attention to the case of periodic clusters, which play an important role at large couplings, see [12–15,25,26]. Stability and bifurcations of spatially homogeneous and clustered periodic solutions of coupled systems have been also studied in Refs. [27–30]. A particular case of the cluster-splitting cascade, cluster doubling, has also been demonstrated in Ref. [14] for a system of globally coupled logistic maps and for systems of globally coupled Duffing oscillators and Josephson junction series arrays.

The starting point in the consideration of cluster-splitting is the investigation of stability of a cluster state. The system of N coupled maps (1) has a stable K -cluster state with the distribution of the oscillators among the clusters $N_1 : N_2 : \dots : N_K$ if the following conditions are fulfilled:

- (i) K -dimensional in-cluster system (3) has an attractor $A^{(K)}$;
- (ii) in-cluster attractor $A^{(K)}$ is also an attractor of the original N -dimensional system (1).

For the condition (ii) to be fulfilled, K transverse Lyapunov exponents [25,31]

$$\lambda_{\perp,j}^{(K)} = \lim_{k \rightarrow \infty} \frac{1}{k} \sum_{n=0}^{k-1} \ln |f'(y_j(n))| + \ln |1-\varepsilon|, \quad j = 1, 2, \dots, K \tag{4}$$

of $A^{(K)}$ must be negative [32]. Note, that each Lyapunov exponent $\lambda_{\perp,j}^{(K)}$ is of multiplicity $N_j - 1$. It is responsible for growth of perturbations destroying the identity of the elements of the j th cluster. Thus, the splitting of the j th cluster is governed by the LE $\lambda_{\perp,j}^{(K)}$.

In this paper, we study mechanisms of cluster-splitting transitions of periodic regimes in system (1). We show that the transition can typically proceed via one of the two following local bifurcations of a stable periodic in-cluster orbit: Transverse period-doubling or transverse transcritical bifurcations. Under these bifurcations, one of the clusters splits

into two stable sub-clusters, thus the total number of clusters increases by one. We observe characteristic cascades of such cluster-splitting bifurcations and conclude that the type of the next splitting bifurcation essentially depends on the form of the previous splitting.

2. Cluster splitting: numerical observation

In this section, we describe how the cluster-splitting transitions appear in numerical experiments. A detailed description and the theory will be presented in the sections below.

Consider system (1) of $N = 100$ coupled logistic maps $f(x) = ax(1 - x)$ with the nonlinearity parameter a and $x \in [0; 1]$. Choose the parameter value $a = 3.84$ providing that the map f has an attracting period-3 cycle γ_3 (its multiplier is equal to $\nu \approx -0.8753$). The symmetric period-3 cycle $\gamma_3^{(1)}$ (originated by the cycle γ_3) belonging to the main diagonal D_N forms a coherent (one-cluster) state which will be stable in the whole N -dimensional phase space if transverse multiplier $\mu_1^{(1)} = \nu(1 - \varepsilon)^3$ calculated in accordance with (4) is less than 1 in absolute value. It can be easily found that this happens for a range of the coupling parameter $\varepsilon \in (\varepsilon^-; \varepsilon^+)$, where $\varepsilon^- \approx -0.0454$ and $\varepsilon^+ \approx 2.0454$. Thus, for this range of ε , system (1) has the asymptotically stable coherent state with period-3 temporal dynamics.

With decreasing ε beyond ε^- , the transverse multiplier $\mu_1^{(1)}$ of $\gamma_3^{(1)}$ becomes less than -1 and the coherent state loses its stability. Just after the bifurcation, system (1) demonstrates a variety of two-cluster states with different ratios of cluster sizes $N_1 : N_2$ and with period-6 temporal dynamics. At further decreasing ε , these clustered states appear to split again in a similar period-doubling way.

In Fig. 1, we plot one-parameter bifurcation diagrams originated from the stable period-3 coherent state of system (1) following the evolution of the dynamics as the coupling parameter ε decreases. At each new value of ε , the initial conditions were slightly randomly perturbed from the asymptotic state of the previous value, and then iterated according to (1) without perturbations. In this way, we trace the evolution of the clustered state in system (1) as ε decreases.¹

Four particular examples of cluster-splitting cascades are presented in Fig. 1. As we can see, the bifurcation sequences can run in different ways, which depends essentially on perturbations described above. In Fig. 1, $CkPm(N_1 : N_2 : \dots : N_k)$ denotes a stable k -cluster state with period- m temporal dynamics and with N_j elements in the j th cluster ($CkQm$ states for superposition of a period- m cycle with quasiperiodic dynamics). The following cluster-splitting sequences are obtained:

Fig. 1a: $C1P3(100) \Rightarrow C2P6(49:51) \Rightarrow C3P12(23:26:51) \Rightarrow C4P12(23:26:21:30)$
 $\Rightarrow C5P24(11:12:26:21:30) \Rightarrow C6P48(5:6:12:26:21:30)$.

Fig. 1b: $C1P3(100) \Rightarrow C2P6(50:50) \Rightarrow C4P12(24:26:25:25) \Rightarrow C4Q12(24:26:25:25)$.

Fig. 1c: $C1P3(100) \Rightarrow C2P6(47:53) \Rightarrow C3P12(23:24:53) \Rightarrow C4P24(10:13:24:53)$
 $\Rightarrow C5P24(10:13:24:19:34) \Rightarrow C6P24(10:13:3:21:19:34) \Rightarrow C7P48(5:5:13:3:21:19:34)$
 $\Rightarrow C9P96(2:3:2:3:13:3:21:19:34)$.

Fig. 1d: $C1P3(100) \Rightarrow C2P6(46:54) \Rightarrow C3P12(23:23:54) \Rightarrow C5P24(11:12:11:12:54)$
 $\Rightarrow C5Q24(11:12:11:12:54)$.

Note that the number of clusters can grow by 1 or by 2, moreover, with or without temporal period-doubling. In one of the cases the cluster-splitting cascade carries on up to nine-cluster states (Fig. 1c). In other cases, it is terminated by four-cluster quasiperiodic dynamics (Fig. 1b).

¹ In this way we consider the clustered states that “smoothly” appear in cluster-splitting bifurcations as ε decreases slowly. It is worth noticing that system (1) may also have many other stable two-cluster states coexisting with those obtained in the calculations.

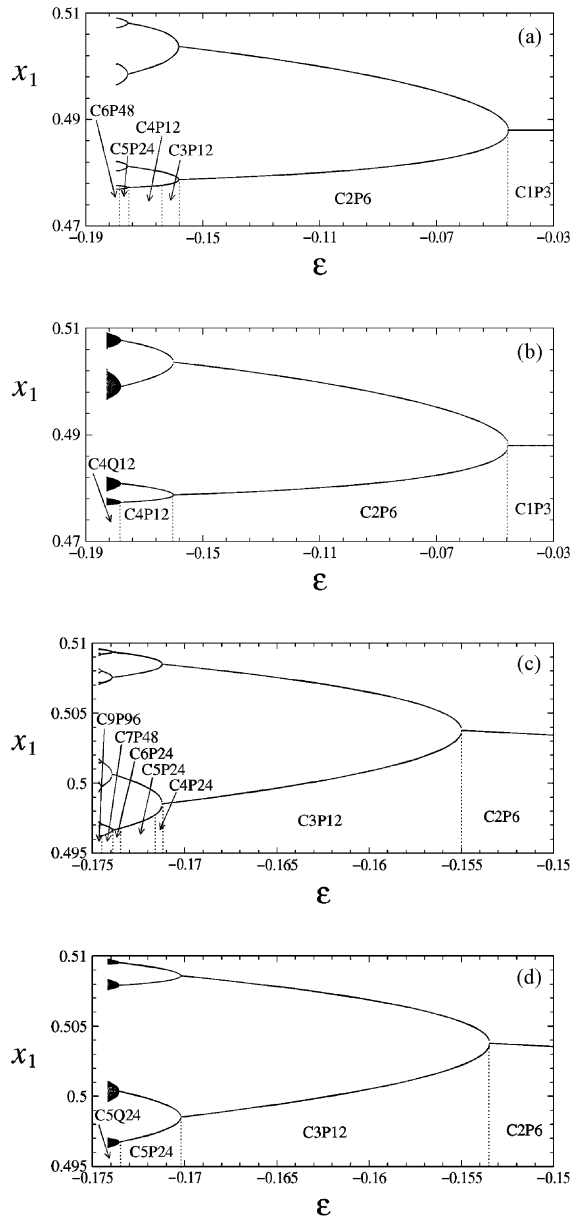


Fig. 1. Bifurcation diagrams for system (1) with $N = 100$ and $a = 3.84$. The only one branch of the original coherent periodic cycle is shown. When calculating, small random perturbations of the amplitude 10^{-9} were applied to the initial conditions at each next value of ϵ .

3. From coherent to two-cluster state: analytical approach

In this section, we present a complete analytic description of cluster-splitting bifurcation for the simplest case of the splitting of period-1 1-cluster to a period-2 2-cluster. Although more complex transitions can be, in principle, handled in a similar way, the corresponding calculations are rather tedious.

We start with the situation when the fixed point $x^* = 1 - 1/a$ of the logistic map $f(x) = ax(1 - x)$ is stable, i.e., its multiplier $v = (2 - a)$ is less than 1 in absolute value. The symmetric fixed point $\gamma_1^{(1)} = (x^*, x^*) \in \Pi_2$ is also stable transversally if $\varepsilon \in (\varepsilon^-; \varepsilon^+)$, where $\varepsilon^\pm = 1 \mp 1/(2 - a)$, i.e., its transverse multiplier $\mu_1^{(1)} = (2 - a)(1 - \varepsilon)$ derived in accordance with (4) is less than 1 in absolute value. We consider below the case $2 < a < 3$, then the transverse multiplier of the fixed point (x^*, x^*) is equal to -1 at $\varepsilon = \varepsilon^- = (3 - a)/(2 - a)$.

To find what happens at this transition we consider the map which acts within the two-cluster subspace Π_2 of the form (3):

$$F_2 : \begin{pmatrix} x \\ y \end{pmatrix} \mapsto \begin{pmatrix} f(x) + (1 - p)\varepsilon(f(y) - f(x)) \\ f(y) + p\varepsilon(f(x) - f(y)) \end{pmatrix}, \quad (5)$$

where $p = p_1^{(2)}$ and $1 - p = p_2^{(2)}$. Each stable regime in this map for $\varepsilon \lesssim \varepsilon^-$ corresponds to a possible cluster-splitting.

3.1. Symmetric splitting

Let $p = 1/2$ (symmetric, i.e., equally sized, two clusters). For $\varepsilon < \varepsilon^-$, the map F_2 has period-2 cycle $\gamma_2^{(2)} = \{(x_1, y_1), (x_2, y_2)\}$ out of the diagonal $D_2 = \{(x, y) | x = y\}$ and such that $x_1 = y_2$ and $x_2 = y_1$ with coordinates

$$x_{1,2} = \frac{a(1 - \varepsilon) + 1 \pm \sqrt{a(a - 2)(1 - \varepsilon)^2 + 2\varepsilon - 3}}{2a(1 - \varepsilon)}.$$

The cycle $\gamma_2^{(2)}$ is stable for the map F_2 , i.e., within the two-cluster subspace Π_2 , for $\varepsilon \in (\varepsilon_h; \varepsilon^-)$, where

$$\varepsilon_h = \frac{2a^2 - 4a - 3 - \sqrt{8a^2 - 16a + 9}}{2a(a - 2)}$$

is a moment of supercritical Hopf bifurcation of $\gamma_2^{(2)}$.

The two transverse multipliers $\mu_{1,2}^{(2)}$ of the symmetric two-cluster state given by the cycle $\gamma_2^{(2)} \in \Pi_2$ are equal to each other (cf. (4))

$$\mu_{1,2}^{(2)} = f'(x_1)f'(x_2)(1 - \varepsilon)^2 = f'(y_1)f'(y_2)(1 - \varepsilon)^2 = a(2 - a)\varepsilon^2 + 2(a^2 - 2a - 1)\varepsilon - a^2 + 2a + 4.$$

Then, one can easily find that the in-cluster cycle $\gamma_2^{(2)} \in \Pi_2$ will be stable in the whole N -dimensional phase space of system (1) if $\varepsilon \in (\varepsilon_{db}; \varepsilon^-)$, where

$$\varepsilon_{db} = \frac{a^2 - 2a - 1 - \sqrt{3a^2 - 6a + 1}}{a(a - 2)}.$$

At $\varepsilon = \varepsilon_{db}$, we have $\mu_{1,2}^{(2)} = -1$, and $\mu_{1,2}^{(2)} < -1$ for $\varepsilon < \varepsilon_{db}$. We can observe that $\varepsilon_h < \varepsilon_{db} < \varepsilon^-$, i.e., splitting occurs prior to the change of the 2-cluster dynamics.

The evolution of the system for $p = 1/2$ can be described as follows. Let us fix $\varepsilon > \varepsilon^-$ in system (1) and start to decrease it. First, the coherent (one-cluster) state given by the fixed point $\gamma_1^{(1)}$ symmetrically (i.e., equally sized) split at $\varepsilon = \varepsilon^-$ into stable two-cluster state given by $\gamma_2^{(2)}$ with doubling temporal periodicity. Then, at $\varepsilon = \varepsilon_{db}$, the two-cluster state loses its stability. In-cluster cycle $\gamma_2^{(2)}$, being stable within the cluster subspace Π_2 , bifurcates via transverse period-doubling bifurcation leading to further cluster-splitting transitions.

3.2. Completely asymmetric splitting

Let $p = 0$ (another limiting case of the system (5)).

As before, the fixed point $\gamma_1^{(1)} = (x^*, x^*)$ of the map F_2 bifurcates with decreasing ε at the same value $\varepsilon = \varepsilon^-$ via transverse period-doubling bifurcation giving birth to a period-2 cycle $\gamma_2^{(2)} = \{(x_1, y_1), (x_2, y_2)\}$

$$x_{1,2} = \frac{a(1 - \varepsilon) + 1 \pm \sqrt{(a - 1)^2(a - \varepsilon)^2 + \varepsilon(1 - \varepsilon)(2a - 3) + \varepsilon - 4}}{2a(1 - \varepsilon)}, \quad y_{1,2} = 1 - \frac{1}{a},$$

which is stable for system (5).

The transverse multiplier $\mu_2^{(2)} = f'(y_1)f'(y_2)(1 - \varepsilon)^2$ of the cycle $\gamma_2^{(2)}$ equals $(2 - a)^2(1 - \varepsilon)^2$ and, consequently, monotonically grows from 1 as ε decreases beyond ε^- . Therefore, in the case $p = 0$, the cycle $\gamma_2^{(2)}$ is born to be transversely unstable.

3.3. General case

To study intermediate cluster splitting, i.e., when $0 < p < 1/2$, we change the variables

$$\xi = \frac{y + x}{2}, \quad \eta = \frac{y - x}{2} \tag{6}$$

transforming the map F_2 into

$$\tilde{F}_2 : \begin{pmatrix} \xi \\ \eta \end{pmatrix} \mapsto \begin{pmatrix} f(\xi) + \varepsilon(1 - 2p)f'(\xi)\eta - a\eta^2 \\ f'(\xi)(1 - \varepsilon)\eta \end{pmatrix}. \tag{7}$$

For $\varepsilon \leq \varepsilon^-$, there exists a one-dimensional invariant unstable manifold $W^u = \{(\xi, \eta) | \xi = \varphi(\eta)\}$ of the symmetric fixed point $(x^*, 0)$ of the map \tilde{F}_2 . The Taylor series expansion of $\varphi(\cdot)$ in the vicinity of zero is

$$\varphi(\eta) = x^* + (2p - 1)\eta + \frac{4ap(1 - p)}{2 - a - (2 - a)^2(1 - \varepsilon)^2}\eta^2 + O(|\eta|^3). \tag{8}$$

Substituting expression (8) into Eq. (7), we obtain a one-dimensional map acting along the manifold W^u (here, we consider only the terms up to the third order)

$$h : \eta \mapsto (2 - a)(1 - \varepsilon)\eta + 2a(1 - 2p)(1 - \varepsilon)\eta^2 + \frac{8a^2p(1 - p)(1 - \varepsilon)}{(2 - a)^2(1 - \varepsilon)^2 + a - 2}\eta^3. \tag{9}$$

The polynomial variable change

$$\eta = g(\theta) = \theta + b\theta^2, \quad b = \frac{2a(1 - 2p)}{(2 - a)^2(1 - \varepsilon)^2 + a - 2} \tag{10}$$

removes the quadratic term in (9), and we obtain the following map (neglecting again terms of high order):

$$\tilde{h} : \theta \mapsto (2 - a)(1 - \varepsilon)\theta + 8a^2(1 - \varepsilon) \left(\frac{(1 - 2p)^2}{(2 - a)((2 - a)(1 - \varepsilon) - 1)} + \frac{p(1 - p)}{(2 - a)^2(1 - \varepsilon)^2 + a - 2} \right) \theta^3.$$

The fixed point $\theta = 0$ of the map \tilde{h} undergoes at $\varepsilon = \varepsilon^-$ a supercritical period-doubling bifurcation giving birth to a stable period-2 cycle whose coordinates are $\theta_{1,2} = \pm\sqrt{q}/r$, where

$$q = 2(2 - a)(1 - \varepsilon)((2 - a)(1 - \varepsilon)^2 - 1)((2 - a)^2(1 - \varepsilon)^2 - 1) \times [p(1 - p)((2 - a)(1 - \varepsilon)(3 - 4\varepsilon) - 3) - (2 - a)(1 - \varepsilon)^2 + 1]$$

and

$$r = 4a(1 - \varepsilon)[p(1 - p)((2 - a)(1 - \varepsilon)(3 - 4\varepsilon) - 3) + (2 - a)(1 - \varepsilon)^2 - 1].$$

Applying the variable change (10), we obtain expressions for coordinates $\eta_{1,2}$ of the corresponding period-2 cycle of the map h

$$\eta_{1,2} = \frac{bq \pm r\sqrt{q}}{r^2}.$$

By using the variable change (6), we can rewrite the maximal transverse multiplier $\mu_2^{(2)} = f'(y_1)f'(y_2)(1 - \varepsilon)^2$ of the cycle $\gamma_2^{(2)}$ of the map F_2 in the form

$$\mu_2^{(2)} = 1 + 4a^2(1 - \varepsilon)^2\eta_1\eta_2 - \frac{2a(1 - \varepsilon)(\eta_1^3 + \eta_2^3)}{\eta_1\eta_2}. \tag{11}$$

Substituting the expressions for $\eta_{1,2}$ in (11), we can obtain the transverse multiplier $\mu_2^{(2)}$ as a function of a , p , and ε : $\mu_2^{(2)} = \mu_2^{(2)}(a, p, \varepsilon)$.

Next, consider a partial derivative of $\mu_2^{(2)}$ with respect to ε at the bifurcation value $\varepsilon = \varepsilon^-$:

$$\left. \frac{\partial \mu_2^{(2)}}{\partial \varepsilon} \right|_{\varepsilon=\varepsilon^-} = \frac{2(a - 1)(a - 2)(3p - 1)}{2ap(p - 1) + a - 1}. \tag{12}$$

For $2 < a < 3$, the derivative (12) equals 0 at $p = 1/3$ and it is negative for $p < 1/3$ and positive for $p > 1/3$. At $\varepsilon = \varepsilon^-$, we have $\mu_2^{(2)} = 1$. Hence, for $p \in [0; 1/3)$, $\mu_2^{(2)}$ grows from 1 as ε starts to decrease from ε^- ; for these values of p the periodic 2-cluster orbit is transversally unstable. Alternatively, for $p \in [1/3; 2/3]$, $\mu_2^{(2)}$ decreases from 1 as ε decreases from ε^- ; for these values of p the periodic 2-cluster orbit is transversally stable. The graphs of the transverse multiplier $\mu_2^{(2)}$ of the two-cluster period-2 cycle $\gamma_2^{(2)}$ are plotted in Fig. 2 for different values of parameter $p = N_1/N$.

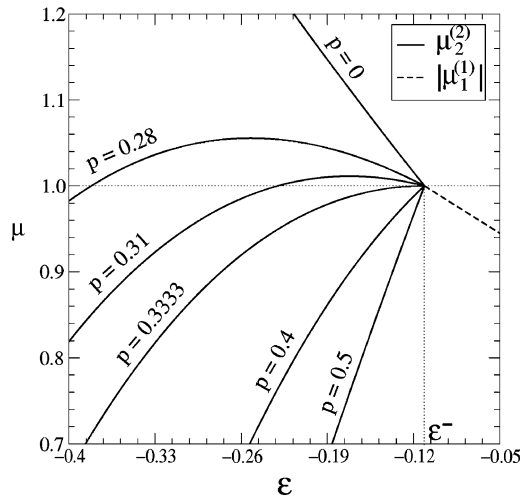


Fig. 2. Solid curves present graphs of the maximal transverse multiplier $\mu_2^{(2)}$ of the two-cluster period-2 cycle $\gamma_2^{(2)}$ for different cluster partitions $p = N_1/N$. Only cycles with $p > 1/3$ are born stable. The dashed curve gives the absolute value of the transverse multiplier of the period-1 coherent state. Parameter $a = 2.9$.

The results above allow us to conclude that the transverse period-doubling bifurcation of the period-1 coherent state of system of N coupled maps (1) can lead to the emergence of stable period-2 two-cluster states, provided that the distribution between the clusters $N_1 : N_2$ satisfies $N_i/N \geq 1/3$, $i = 1, 2$, or, equivalently, $1/2 \leq N_1/N_2 \leq 2$. Below we shall see that the critical ratio $N_1/N_2 = 1/2$ holds also for other cluster-splitting bifurcations induced by other in-cluster cycles.

4. Two mechanisms of cluster splitting: period-doubling and transcritical

In this section, we describe two mechanisms of cluster-splitting transitions that occur in system (1) when parameter ε decreases.

Suppose that system (1) has a stable $CkPm(N_1 : N_2 : \dots : N_K)$ -state, i.e., a K -cluster state with period- m temporal dynamics and with the variable distribution among the clusters of the form $N_1 : N_2 : \dots : N_K$. In this case, the system F_K of the form (3) with parameters $\{p_i^{(K)}\}_{i=1}^K$, $p_i^{(K)} = N_i/N$, has a stable period- m cycle $\gamma_m^{(K)}$. In-cluster stability (i.e., stability with respect to the K -dimensional system F_K) of this cycle is determined by K in-cluster multipliers $v_i^{(K)}$, $i = \overline{1, K}$. The other set of K transverse multipliers $\mu_i^{(K)}$, $i = \overline{1, K}$, calculated in accordance with (4) control the transverse stability (i.e., stability with respect to out-cluster perturbations) of $\gamma_m^{(K)}$. The cycle $\gamma_m^{(K)}$ provides a stable K -cluster states if all multipliers $v_i^{(K)}$ and $\mu_i^{(K)}$, $i = \overline{1, K}$, are less than 1 in absolute value.

When the parameters a and ε of system (1) vary, the multipliers of $\gamma_m^{(K)}$ may leave the unit disk. In this connection, we distinguish between two typical cases: Either one of the in-cluster multipliers $v_i^{(K)}$ or one of the transverse multipliers $\mu_i^{(K)}$ becomes larger than 1 in absolute value. In the first case, the in-cluster attractor $\gamma_m^{(K)}$ bifurcates within the cluster subspace Π_K changing in-cluster dynamics via, e.g., period-doubling, Hopf, or saddle-node bifurcation. Transversal stability of the cluster state is preserved by continuity, provided that the bifurcation above is supercritical. In the second case, which is a subject of our interest, the in-cluster cycle $\gamma_m^{(K)}$ loses its stability in the transverse to the cluster subspace directions causing, as we shall see, cluster splitting.

Suppose that one of the transverse multipliers $\mu_i^{(K)}$ leaves the interval $[-1; 1]$ as parameters vary² while the others do not; this is a general situation. Below we argue that at this transition the i th cluster of system (1) can split into two clusters. The other clusters remain unaffected as soon as the other transverse multipliers remains inside $[-1; 1]$. To investigate this cluster bifurcation, we consider the $(K + 1)$ -dimensional system F_{K+1} of the form (3) with parameters $\{p_j^{(K+1)}\}_{j=1}^{K+1}$ such that $p_j^{(K+1)} = p_j^{(K)}$ for $j < i$, $p_i^{(K+1)} + p_{i+1}^{(K+1)} = p_i^{(K)}$, and $p_{j+1}^{(K+1)} = p_j^{(K)}$ for $j > i$. In other words, we seek for a solution where the i th cluster splits into two, with still undetermined parameters $p_i^{(K+1)}$ and $p_{i+1}^{(K+1)}$. If this new system F_{K+1} attains a stable cycle $\gamma_q^{(K+1)}$ (which is stable also transversely, i.e., all its $K + 1$ transverse multipliers are less than 1 in absolute value), then system (1) demonstrates a cluster-splitting bifurcation.

In Fig. 3a–c, different mechanisms of cluster-splitting transition are shown schematically. They depend on the value of $\mu_i^{(K)}$ (-1 or $+1$) at the bifurcation: (a) $\mu_i^{(K)}$ passes through -1 , (b) and (c) $\mu_i^{(K)}$ passes through $+1$. The vertical axis depicts the difference η between the two newly split clusters $y_i^{(K+1)}$ and $y_{i+1}^{(K+1)}$. Bold curves correspond to stable clusters, thin ones to unstable clusters.

4.1. Period-doubling splitting

In Fig. 3a, the period-doubling cluster-splitting transition is presented. At $\varepsilon = \varepsilon_{\text{db}}$, the transverse multiplier $\mu_i^{(K)}$ of the K -cluster cycle $\gamma_m^{(K)}$ becomes less than -1 . The period- m cycle $\gamma_m^{(K)}$ undergoes transverse

² For the system (1), the transverse multipliers $\mu_i^{(K)}$ are real as follows from (4), because the coupled maps are one-dimensional.

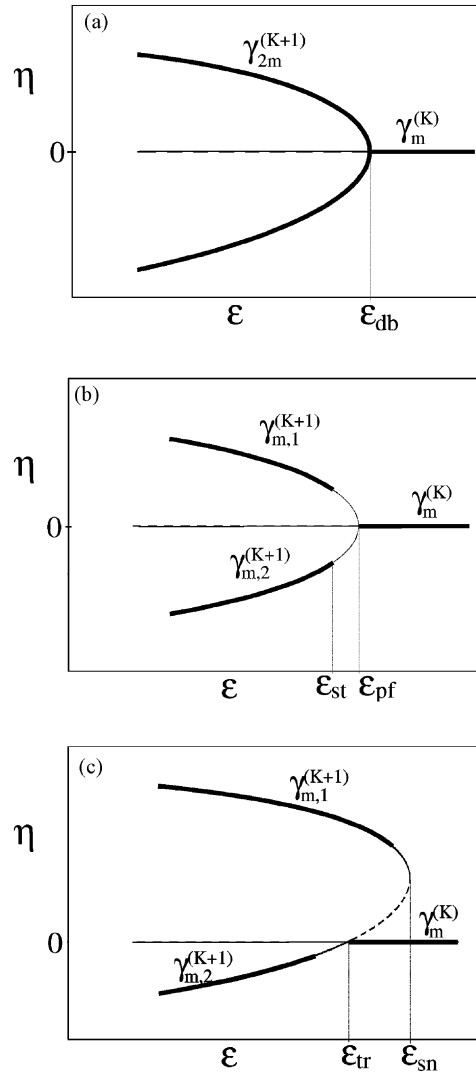


Fig. 3. Different mechanisms of cluster-splitting which proceed (a) via period-doubling, (b) pitchfork, and (c) via transcritical bifurcation. $\eta = y_i^{(K+1)} - y_{i+1}^{(K+1)}$ is a difference between two newly spitted clusters. The thin solid and dashed curves correspond, respectively, to stable and unstable, within the corresponding cluster subspace, in-cluster cycles involved in the bifurcation. The bold solid curves correspond to stable in the whole N -dimensional phase space in-cluster cycles. Transverse pitchfork bifurcation (b) does not instantly lead to cluster stable clusters: They stabilize later at $\varepsilon = \varepsilon_{st}$.

period-doubling bifurcation giving birth to a stable period- $2m$ cycle $\gamma_{2m}^{(K+1)}$ which belongs to a $(K+1)$ -cluster subspace Π_{K+1} . The splitting considered is said to be symmetric if two equal-size clusters $p_i^{(K+1)} = p_{i+1}^{(K+1)} = \frac{1}{2} p_i^{(K)}$ arise, and asymmetric if $p_i^{(K+1)} \neq p_{i+1}^{(K+1)}$. While the in-cluster attractor $\gamma_{2m}^{(K+1)}$ is born to be stable within the cluster subspace Π_{K+1} , the transverse stability of $\gamma_{2m}^{(K+1)}$ depends essentially on the measure of asymmetry, i.e., on the ratio $p_i^{(K+1)}/p_{i+1}^{(K+1)}$. From the consideration of Section 3 it follows that the splitting is stable if $1/2 \leq p_i^{(K+1)}/p_{i+1}^{(K+1)} \leq 2$.

4.2. Pitchfork and transcritical splitting

Another cluster-splitting scenarios occur in system (1) when the transverse multiplier $\mu_i^{(K)}$ of the cycle $\gamma_m^{(K)}$ passes through 1. Then, the cycle $\gamma_m^{(K)}$ loses its transverse stability in pitchfork or transcritical bifurcation depending on whether symmetric or asymmetric splitting occurs (i.e., depending on the ratio $p_i^{(K+1)}/p_{i+1}^{(K+1)}$). Indeed, after the bifurcation, there are two stable period- m cycles $\gamma_{m,1}^{(K+1)}$ and $\gamma_{m,2}^{(K+1)}$ for the corresponding system F_{K+1} . These cycles are born via a transverse pitchfork bifurcation of $\gamma_m^{(K)}$ at $\varepsilon = \varepsilon_{\text{pf}}$ if the splitting is symmetric ($p_i^{(K+1)} = p_{i+1}^{(K+1)}$, Fig. 3b). If the splitting is asymmetric ($p_i^{(K+1)} \neq p_{i+1}^{(K+1)}$), the cycles $\gamma_{m,1}^{(K+1)}$ and $\gamma_{m,2}^{(K+1)}$ are born in a saddle-node bifurcation at $\varepsilon = \varepsilon_{\text{sn}}$ followed by a transcritical bifurcation of the cycles $\gamma_m^{(K)}$ and $\gamma_{m,2}^{(K+1)}$ at $\varepsilon = \varepsilon_{\text{tr}} = \varepsilon_{\text{pf}}$ (Fig. 3c, see also Ref. [33]). The transverse stability of the cycles $\gamma_{m,i}^{(K+1)}$, $i = 1, 2$ can be argued as follows. First note that both pitchfork and transcritical bifurcations do not change temporal period. Consider next the pitchfork bifurcation, one can easily see that here when a fixed point moves away from the diagonal in the transverse direction, one of the variables decreases and the other increases. This implies that the transversal exponents corresponding to these variables split: one increases and the other decreases. Thus, one of the new-born clusters will be transversally unstable, which causes the instability of the whole clustered state. The new-born clusters can stabilize in the N -dimensional phase space only at some distance from the bifurcation point (bold curves in Fig. 3b start from $\varepsilon = \varepsilon_{\text{st}} < \varepsilon^-$). At the transcritical bifurcation, where one branch lies far away from the bifurcating solution, different variants are possible. Fig. 3c demonstrates one possibility, where the cycle $\gamma_{m,2}^{(K+1)}$ becomes transversely stable at a distance from the transcritical destabilization of $\gamma_m^{(K)}$, whereas the other cycle $\gamma_{m,1}^{(K+1)}$ can be transversely stable even prior to the transcritical bifurcation (bold curves in Fig. 3c). In this case, the transverse transcritical bifurcation of a periodic K -cluster attractor leads to an asymmetric cluster-splitting without change of temporal periodicity.

5. Cluster-splitting cascades

In this section, we follow the cluster-splitting cascades presented in Fig. 1 and describe in detail the mechanisms of the cluster-splitting bifurcations outlined in the previous section. As in Section 2, we fix parameter value $a = 3.84$ at which logistic map f_a has a stable period-3 cycle. We expect the bifurcation properties to be qualitatively similar for other periodic windows of f .

5.1. Cluster-splitting via period-doubling

Consider the two-dimensional system F_2 of the form (3) (i.e., $K = 2$ there) having two parameters $p_1^{(2)}$ and $p_2^{(2)} = 1 - p_1^{(2)}$. Suppose, for definiteness, that $p_1^{(2)} \leq 1/2$, i.e., the first of the two clusters is not larger of the second one. For any $\varepsilon \in (\varepsilon^-; \varepsilon^+)$ (ε^\pm are such as in Section 2), system F_2 has a stable period-3 cycle $\gamma_3^{(1)}$ on the diagonal $D_2 = \{(y_1, y_2) | y_1 = y_2\}$. At $\varepsilon = \varepsilon^-$, the cycle $\gamma_3^{(1)}$ undergoes a transverse supercritical period-doubling bifurcation (multiplier $\mu_1^{(1)}$ passes through -1) giving birth to a stable period-6 cycle $\gamma_6^{(2)}$ which splits from the diagonal D_2 as ε further decreases.

In Fig. 4, the bifurcation diagram in the $(p_1^{(2)}, \varepsilon)$ -parameter plane is presented. The region of the in-cluster stability of $\gamma_6^{(2)}$ is obliquely hatched. It contains two sub-regions: $C2P6^U$ and $C2P6^S$. In the region $C2P6^S$, which is shaded by dark gray, both transverse multipliers $\mu_1^{(2)}$ and $\mu_2^{(2)}$ of the cycle $\gamma_6^{(2)}$ are less than 1 in absolute value, i.e., this state is transversally stable. The transition at $\varepsilon = \varepsilon^-$ is an example of the cluster-splitting via period-doubling, as described in Section 4.

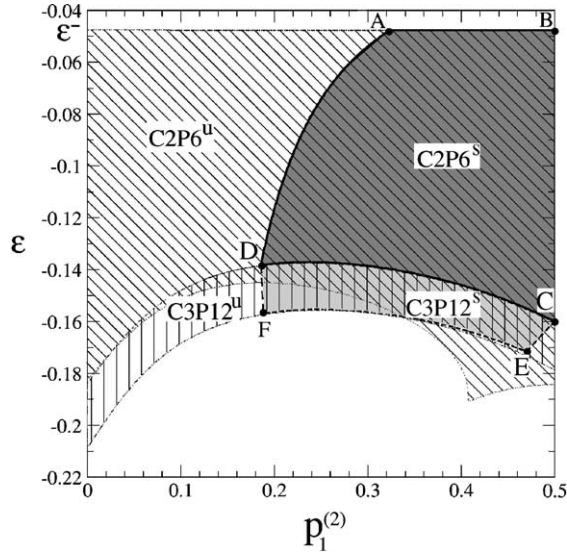


Fig. 4. Cluster-splitting bifurcation diagram for the coherent (one-cluster) state of system (1). The dark gray domain ABCD is the stability region of two-cluster states with period-6 temporal dynamics and partition $\{p_1^{(2)}, p_2^{(2)}\}$. The light gray domain DCEF is the stability region of three-cluster period-12 states with partition $\{p_1^{(3)}, p_2^{(3)}, p_3^{(3)}\}$, where $p_1^{(3)} = p_2^{(3)} = \frac{1}{2} p_1^{(2)}$ and $p_3^{(3)} = p_2^{(2)}$. Obliquely and vertically hatched regions are for the stability of the two- and three-cluster periodic attractors within the corresponding cluster subspaces, respectively. Parameter $a = 3.84$.

Although, in general, all values of $p_1^{(2)}$ are possible, their relative probabilities are different, as shown in Fig. 5. From the numerical experiments it follows that the most probable clusters to be captured at direct numerical simulations with randomly distributed initial conditions are close to symmetric ones. If all partitions of elements in two clusters were equally probable (equipartition), then the probabilities would be equal to the total number of different two-cluster states, i.e., to $N!/(N_1!N_2!)$. Asymptotically for large N , with the use of Stirling formula, this distribution density can be written as $\mathcal{P}(p_1^{(2)}) \sim \exp(N[-p_1^{(2)} \ln p_1^{(2)} - (1 - p_1^{(2)}) \ln(1 - p_1^{(2)})])$. However, this simple estimation does not work (see Fig. 5b). In numerical experiments we indeed observe that for large N the probability density scales as $\mathcal{P}(p_1^{(2)}) \sim \exp(N\phi(p_1^{(2)}))$, but the function ϕ is much stronger concentrated near symmetric partition than one gets from the equipartition. One can conclude that the nearly symmetric clusters have much larger basin of attraction in the whole N -dimensional phase space comparing to non-symmetric ones.

If ε further decreases beyond the bifurcation value $\varepsilon = \varepsilon^-$, the $(p_1^{(2)}, \varepsilon)$ -parameter point leaves the region $C2P6^S$ through its lower boundary, curve DC in Fig. 4. The transverse multiplier $\mu_1^{(2)}$ of the period-6 cycle $\gamma_6^{(2)}$ (or both the transverse multipliers $\mu_1^{(2)}$ and $\mu_2^{(2)}$ if $p_1^{(2)} = 1/2$, point C in Fig. 4) becomes less than -1 . Here the next cluster-splitting period-doubling bifurcation occurs; its features can be analyzed analogously to the consideration above.

To evaluate stability of the new-born clusters, consider the system F_3 of the form (3) with $K = 3$. There are three parameters $p_i^{(3)}$, $i = \overline{1, 3}$ such that $p_1^{(3)} + p_2^{(3)} + p_3^{(3)} = 1$. Consider the case $p_1^{(3)} = p_2^{(3)} (= \frac{1}{2} p_1^{(2)})$ and $p_3^{(3)} = p_2^{(2)}$, i.e., the case where in the two-cluster state $(p_1^{(2)}, p_2^{(2)})$ the first cluster splits into two equal parts. First, in $(p_1^{(3)} + p_2^{(3)}, \varepsilon)$ -parameter plane, we find a region, where system F_3 has a stable period-12 cycle $\gamma_{12}^{(3)}$. In Fig. 4, this region is vertically hatched being delineated by two thin dot-dashed curves. It contains a sub-region $C3P12^S$, where the cycle $\gamma_{12}^{(3)}$ is stable in N dimensions so as, in addition, all three transverse multipliers $\mu_i^{(3)}$, $i = \overline{1, 3}$ of $\gamma_{12}^{(3)}$ are less than 1 in absolute value. This region $C3P12^S$ is shaded by light gray in Fig. 4 and bounded by

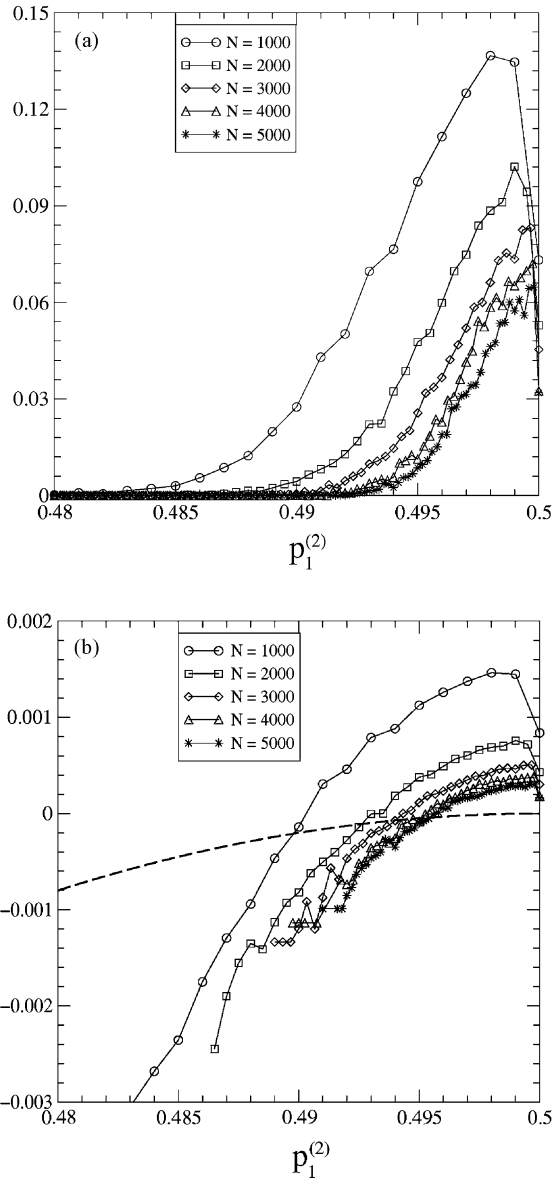


Fig. 5. (a) Probability for a trajectory of system (1) to be attracted by a two-cluster state with partition $\{p_1^{(2)}, p_2^{(2)}\}$ after transverse destabilization the coherent state. The average has been done over 10,000 initial conditions randomly distributed in a small neighborhood (diameter is 10^{-9}) of the unstable coherent state for ε slightly beyond its transverse period-doubling bifurcation. Parameter $a = 3.84$. (b) The same probabilities as densities in the scaled coordinates, where the vertical axis represents $(\ln \mathcal{P} - 0.5 \ln N)/N$, to reveal the scaling behavior for large N . The scaling distribution resulting from the equipartition hypothesis is shown with dashed curve.

bold dashed curves. One can see that the regions $C2P6^S$ and $C3P12^S$ are fitted each to other along the arc DC. Therefore, the transverse period-doubling bifurcation of the two-cluster period-6 cycle $\gamma_6^{(2)}$ induces cluster splitting of one of the two clusters leading to the appearance of stable three-cluster states of double temporal periodicity.

If $p_1^{(2)} < p_2^{(2)}$ (the case $p_1^{(2)} = p_2^{(2)}$ will be consider later in Section 5.3), then the smaller $p_1^{(2)}$ -cluster of the two-cluster state splits into two sub-clusters. After the bifurcation, system (1) has stable three-cluster states

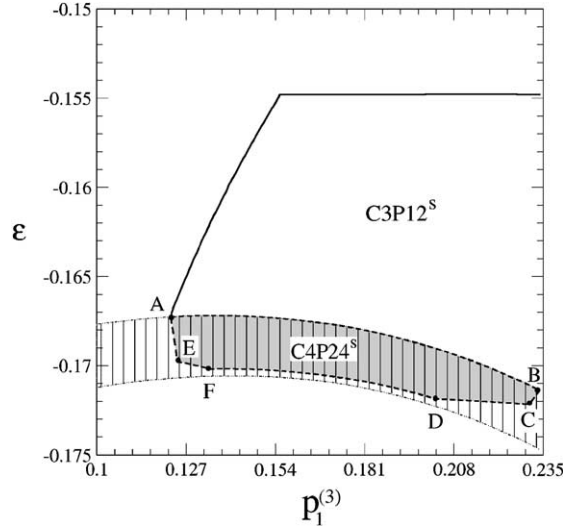


Fig. 6. Cluster-splitting bifurcation diagram of a three-cluster state. $C3P12^S$ is a stability regions for period-12 three-cluster states with a partition $\{p_i^{(3)}\}_{i=1}^3$ such that $p_3^{(3)} = 0.532$ is fixed ($p_1^{(3)} + p_2^{(3)} = 0.468$). $C4P24^S$ is a stability region for period-24 four-cluster states with partition $\{p_i^{(4)}\}_{i=1}^4$ such that $p_1^{(4)} = p_2^{(4)} = \frac{1}{2}p_1^{(3)}$, $p_3^{(4)} = p_2^{(3)}$, and $p_4^{(4)} = p_3^{(3)}$. Parameter $a = 3.84$.

with variables distribution among the clusters of the form $p_1^{(3)}N : p_2^{(3)}N : p_3^{(3)}N$, where $p_1^{(3)} + p_2^{(3)} = p_1^{(2)}$ and $p_3^{(3)} = p_2^{(2)}$. Splitting is symmetric if $p_1^{(3)} = p_2^{(3)}$ (Fig. 4).

In Fig. 6, the region of stability of three-cluster states, denoted by $C3P12^S$, is presented for the case $p_1^{(3)} \leq p_2^{(3)}$, where the sum $p_1^{(3)} + p_2^{(3)} = p_1^{(2)}$ is fixed, i.e., when the three-cluster states are born in period-doubling splitting of a two-cluster state with some fixed partition $\{p_1^{(2)}, 1 - p_1^{(2)}\}$. As one can conclude, the cluster-splitting bifurcation of the two-cluster state runs in the same way as for the coherent (one-cluster) state. It results in a variety of stable three-cluster states of period-12 temporal periodicity. In this case, the $p_1^{(2)}$ -cluster can split via period-doubling into either two equal sub-clusters $p_1^{(3)} = p_2^{(3)}$ (symmetric splitting) or non-equal sub-clusters $p_1^{(3)} < p_2^{(3)}$ (asymmetric splitting).

With further decrease of the coupling parameter ε , the parameter point on the plane $(p_1^{(3)}, \varepsilon)$ leaves region $C3P12^S$ through its lower boundary (the bifurcation curve FEC in Fig. 4 or the curve AB in Fig. 6). The three-cluster attractor $\gamma_{12}^{(3)}$ losses its stability in transverse to the cluster subspace Π_3 directions. Depending on the values of the parameters $p_i^{(3)}$, the transverse bifurcation of $\gamma_{12}^{(3)}$ may develop differently as it is demonstrated in Fig. 3a and c. There are two possibilities related to two arcs FE and EC of the bifurcation curve FEC bounding the region $C3P12^S$ from below in Fig. 4. The critical bifurcation value for the parameter $p_1^{(2)} = p_1^{(3)} + p_2^{(3)}$ is given by the point E for which $p_1^{(2)} \approx 0.47$. Then clearly $p_3^{(3)} \approx 0.53$.

Consider first the case $p_1^{(2)} < 0.47$, then $p_3^{(3)} > 0.53$. For $p_3^{(3)} = 0.532$, the stability region $C3P12^S$ of the three-cluster periodic attractor $\gamma_{12}^{(3)}$ is delineated by solid bold curves in Fig. 6. Along the bifurcation curve AB, the transverse multiplier $\mu_1^{(3)}$ of the cycle $\gamma_{12}^{(3)}$ (or two multipliers $\mu_1^{(3)}$ and $\mu_2^{(3)}$ if $p_1^{(3)} = p_2^{(3)}$, point B in Fig. 6, this case will be considered later in Section 5.3) becomes equal to -1 . The cycle undergoes transverse period-doubling bifurcation. In addition, it remains stable within the cluster subspace Π_3 . Therefore, we can apply the above-described cluster-splitting procedure for the transition from three to four clusters.

Consider a system F_4 of the form (3) with $K = 4$ and parameters $p_i^{(4)}$, $i = \overline{1, 4}$, such that $p_1^{(4)} = p_2^{(4)} = \frac{1}{2}p_1^{(3)}$, $p_3^{(4)} = p_2^{(3)}$, and $p_4^{(4)} = p_3^{(3)}$. At the transverse period-doubling bifurcation of the cycle $\gamma_{12}^{(3)}$, F_4 attains a stable

period-24 cycle $\gamma_{24}^{(4)}$ (vertically hatched region in $(p_1^{(4)} + p_2^{(4)}, \varepsilon)$ -parameter plane, Fig. 6). For the considered case of symmetric splitting, i.e., $p_1^{(4)} = p_2^{(4)}$, the four-cluster cycle $\gamma_{24}^{(4)}$ is born to be also stable in the whole N -dimensional phase space of system (1). The region $C4P24^S$ of the N -dimensional stability is shaded by light gray in Fig. 6. Thus, we again observe cluster-splitting bifurcation: The $p_1^{(3)}$ -cluster, which is the smallest in the partition $\{p_1^{(3)}, p_2^{(3)}, p_3^{(3)}\}$, splits into two sub-clusters via temporal period-doubling producing stable four-cluster period-24 states.

In the case of asymmetric splitting $p_1^{(4)} \neq p_2^{(4)}$, the transverse stability of the cycle $\gamma_{24}^{(4)}$ depends essentially on the level of asymmetry $p_1^{(4)}/p_2^{(4)}$ between the two newly split sub-clusters. The situation is analogous to that described above for the splitting of coherent and two-cluster states, see Figs. 4 and 6, respectively.

5.2. Transcritical cluster splitting

The transcritical cluster-splitting bifurcation scenario (see Fig. 3c) occurs for the three-cluster state $C3P12$ in the case $p_3^{(3)} < 0.53$. Then $p_1^{(2)} > 0.47$ and the destabilization of $\gamma_{12}^{(3)}$ is caused by crossing the bifurcation curves CE in Fig. 4 by the parameter point $(p_1^{(2)}, \varepsilon)$. Along this bifurcation curve, the transverse multiplier $\mu_3^{(3)}$ of the three-cluster cycle $\gamma_{12}^{(3)}$ is equal to 1, i.e., the $p_3^{(3)}$ -cluster splits as parameter ε decreases via a pitchfork/transcritical bifurcation.

In Fig. 7, we present a typical diagram of this bifurcation for a fixed value $p_3^{(3)} < 0.53$. The multiplier is $\mu_3^{(3)} = 1$ along the bifurcation curve AB. Below the curve, the four-dimensional system F_4 of the form (3) with parameters $p_i^{(4)}$, $i = \overline{1, 4}$, such that $p_1^{(4)} = p_1^{(3)}$, $p_2^{(4)} = p_2^{(3)}$, and $p_3^{(4)} = p_4^{(4)} = \frac{1}{2}p_3^{(3)}$ (symmetric splitting) has two period-12 cycles $\gamma_{12,1}^{(4)}$ and $\gamma_{12,2}^{(4)}$. Both cycles are born in a transverse pitchfork bifurcation of the three-cluster cycle $\gamma_{12}^{(3)}$ and are stable for the system F_4 , i.e., within the cluster subspace Π_4 . In Fig. 7, in-cluster stability region of $\gamma_{12,i}^{(4)}$ is hatched by vertical lines.

Sub-region of the N -dimensional stability of the four-cluster cycles $\gamma_{12,i}^{(4)}$, $i = 1, 2$ is shaded by light gray and denoted by $C4P12^S$ in Fig. 7. As one can see, there is a gap between the bifurcation curves AB and CD in Fig. 7a, where the four-cluster states considered are transversely unstable. The gap becomes less visible as asymmetry between the clusters decreases, see Fig. 7b. Therefore, the transverse pitchfork bifurcation of a periodic in-cluster attractor does not directly results in a stable cluster splitting: All newly born clusters appear first to be unstable. Nevertheless, soon after the bifurcation they stabilize. Cluster-splitting occurs but with “a parameter delay”, see also Fig. 3b.

Consider now the generic case, where the splitting is asymmetric: $p_3^{(4)} + p_4^{(4)} = p_3^{(3)}$, $p_3^{(4)} \leq p_4^{(4)}$. For fixed $p_1^{(4)} = 0.22$ and $p_2^{(4)} = 0.26$, the regions $C4P12_1^S$ and $C4P12_2^S$ of stability in N dimensions of the cycles $\gamma_{12,1}^{(4)}$ and $\gamma_{12,2}^{(4)}$, respectively, are delineated in Fig. 8. In the subplot, the dotted rectangle is enlarged, where the thin dot-dashed horizontal line at the value $\varepsilon_{tr} = -0.167443$ indicates the moment at which the three-cluster period-12 cycle $\gamma_{12}^{(3)}$ loses its transverse stability in a transcritical bifurcation. The three-cluster partition is $\{0.22, 0.26, 0.52\}$.

One can see in Fig. 8 that, at the moment when period-12 three-cluster state $C3P12$ loses its stability in the transcritical bifurcation, the only $\gamma_{12,1}^{(4)}$ cycle can be stable (in N dimensions), which occurs when $p_3^{(4)}$ is smaller than the abscissa of the point F (shown in the subplot). Therefore, the transverse transcritical bifurcation of periodic in-cluster attractor leads to asymmetric cluster splitting as was also observed in Fig. 1a and c.

5.3. Symmetric cluster-splitting

Here we discuss a situation mentioned already in Section 5.1, namely the case, where the coherent period-3 state symmetrically splits into two-cluster states with partition $\{p_1^{(2)}, p_2^{(2)}\}$ such that $p_1^{(2)} = p_2^{(2)} = 1/2$. This splitting

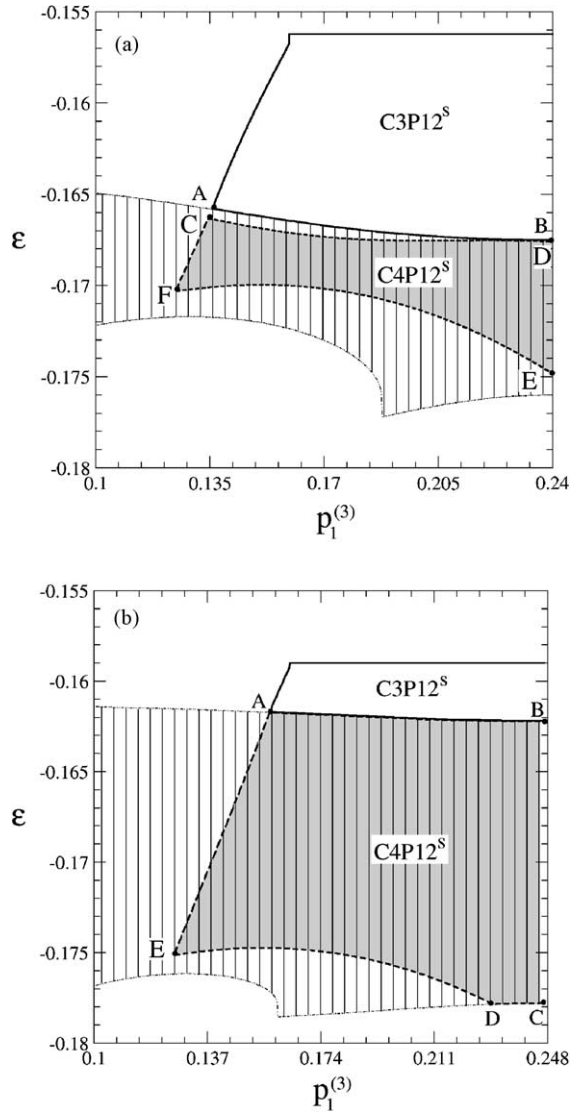


Fig. 7. Cluster-splitting bifurcation diagram for pitchfork transverse destabilization of the generative cycle $\gamma_{12}^{(3)}$. $C3P12^S$ and $C4P12^S$ are stability regions for period-12 three- and four-cluster states with the following partitions: (a) $p_3^{(3)} = 0.52$ is fixed and $p_3^{(4)} = p_4^{(4)} = \frac{1}{2}p_3^{(3)} = 0.26$. (b) $p_3^{(3)} = 0.506$ is fixed and $p_3^{(4)} = p_4^{(4)} = \frac{1}{2}p_3^{(3)} = 0.253$. Parameter $a = 3.84$.

proceeds via temporal period-doubling. After the bifurcation, a stable symmetric period-6 two-cluster states $C2P6$ appears, see Fig. 4. Both the transverse multipliers $\mu_i^{(2)}$, $i = 1, 2$ of $C2P6$ are equal to each other and, with decreasing ϵ , become less than -1 (bifurcation point C in Fig. 4). Therefore, at this bifurcation, both clusters split simultaneously via temporal period-doubling bifurcation giving rise to stable four-cluster states with variable distribution among the clusters $p_1^{(4)}N : p_2^{(4)}N : p_3^{(4)}N : p_4^{(4)}N$, where $p_1^{(4)} + p_2^{(4)} = p_1^{(2)}$ and $p_3^{(4)} + p_4^{(4)} = p_2^{(2)}$. At this transition, each of two clusters $p_i^{(2)}$, $i = 1, 2$, may split symmetrically ($p_i^{(4)} = 1/4$, $i = \overline{1, 4}$) or asymmetrically ($p_i^{(4)} \neq p_j^{(4)}$, $i \neq j$) independently of the splitting of the other cluster. Symmetric splitting is always stable,

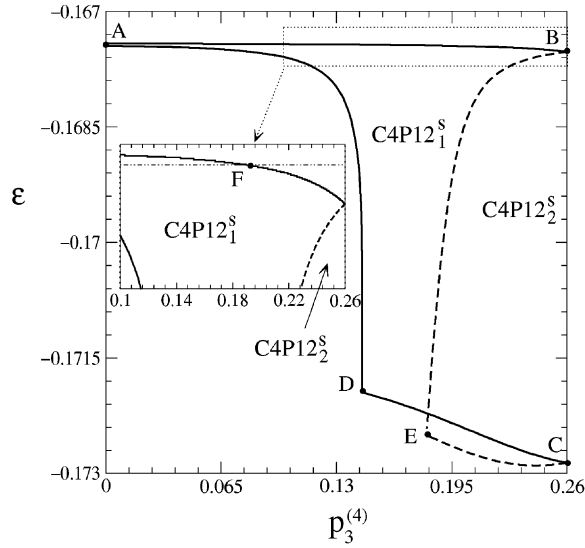


Fig. 8. Stability regions of four-cluster period-12 states of system (1) originated from the cycles $\gamma_{12,1}^{(4)}$ (bounded by bold solid curves) and $\gamma_{12,2}^{(4)}$ (bounded by bold dashed curves). The partition $\{p_i^{(4)}\}_{i=1}^4$ is such that $p_1^{(4)} = 0.22$ and $p_2^{(4)} = 0.26$. Dot-dashed horizontal line in the subplot corresponds to transcritical loss of transverse stability by $C3P12$ -state with partition $\{0.22, 0.26, 0.52\}$. Parameter $a = 3.84$.

whereas the asymmetric splitting is stable if $1/2 \leq p_1^{(4)}/p_2^{(4)} \leq 2$ and $1/2 \leq p_3^{(4)}/p_4^{(4)} \leq 2$. The stability regions of $C4P12$ -states are denoted by $C4P12^S$ in Fig. 9a.

With further decreasing ε , the four-cluster states bifurcate either within its cluster subspace Π_4 via Hopf bifurcation (the bifurcation curve CD in Fig. 9a) or via transverse period-doubling when the cluster $p_1^{(4)}$ (the bifurcation curve DE) or $p_4^{(4)}$ (the bifurcation curve EF) splits, resulting in stable period-24 five-cluster states.

Fig. 9b shows the situation when a period-12 three-cluster state with a distribution among clusters $p_1^{(3)}N : p_2^{(3)}N : p_3^{(3)}N$ such that $p_1^{(3)} = p_2^{(3)}$, bifurcates via transverse period-doubling (the bifurcation curve EF in Fig. 4 or point B in Fig. 6). (Such a three-cluster state has arisen before from the period-6 two-cluster state with partition $\{p_1^{(2)}, p_2^{(2)}\}$ via symmetric period-doubling splitting of the $p_1^{(2)}$ -cluster into two equal sub-clusters $p_1^{(3)} = p_2^{(3)} = \frac{1}{2}p_1^{(2)}$, see Fig. 4, point C.) Then period-24 five-cluster states arise. Their region of stability is presented in Fig. 9b and denoted by $C5P24^S$. Each of these clustered states are born at the moment of loss of transverse stability by the three-cluster states $C3P12$ at $\varepsilon \approx -0.1702$. At the bifurcation, two equal clusters $p_1^{(3)}$ and $p_2^{(3)}$ of $C3P12$ split simultaneously via transverse period-doubling resulting in the appearance of a variety of stable period-24 five-cluster states.

With further decreasing ε , the five-cluster states bifurcate within the cluster subspace via period-doubling (bifurcation curve EF in Fig. 9b) or via Hopf bifurcation (bifurcation curve CD). Moreover, the five-cluster states may also bifurcate with cluster splitting (bifurcation curves DE and FG) when $p_3^{(5)}$ -cluster splits via temporal period-doubling giving birth to stable period-48 six-cluster states.

5.4. Cluster transition tree

We summarize our findings in Fig. 10, where the cluster transitions up to five-cluster states are collected schematically.

With decreasing the coupling parameter ε , the coherent period-3 state $C1P3$ splits into two-cluster states $C2P6$ with partition $\{p_1^{(2)}, p_2^{(2)}\}$ via temporal period-doubling (bifurcation curve AB in Fig. 4, transition I in Fig. 10). The

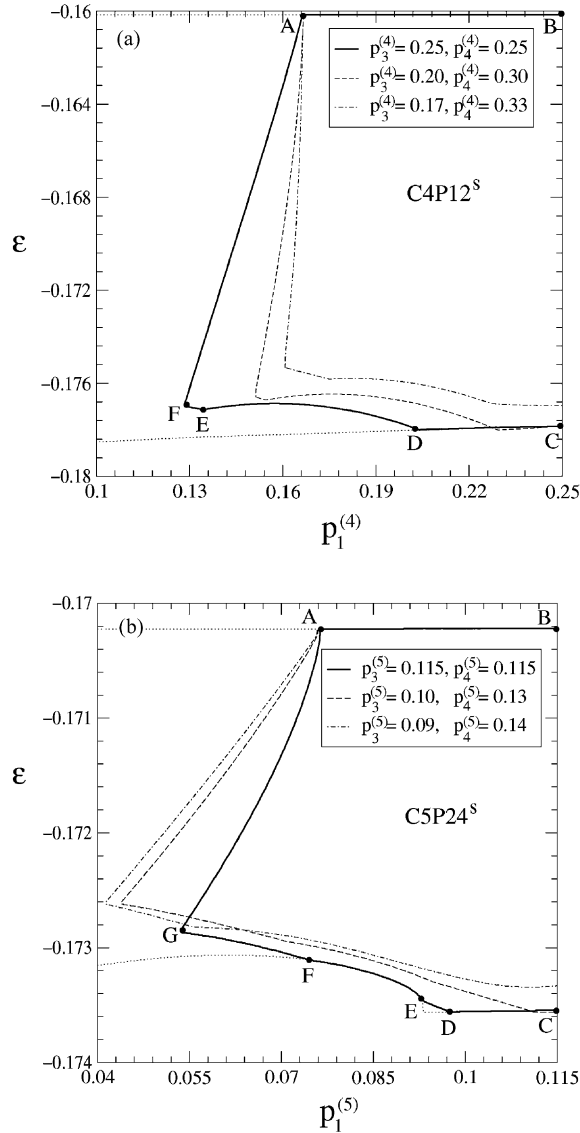


Fig. 9. (a) Stability regions of period-12 four-cluster states with partition $\{p_i^{(4)}\}_{i=1}^4$ that arise after cluster-splitting bifurcation of symmetric period-6 two-cluster state. (b) Stability regions of period-24 five-cluster states with partition $\{p_i^{(5)}\}_{i=1}^5$ that arise after cluster-splitting bifurcation of period-12 three-cluster state with two equal clusters $p_1^{(3)} = p_2^{(3)}$ and with $p_3^{(3)} = 0.54 = p_5^{(3)}$. Parameter $a = 3.84$.

splitting can be symmetric ($p_1^{(2)} = p_2^{(2)}$) or asymmetric ($p_1^{(2)} \neq p_2^{(2)}$). In the latter case, the two-cluster state $C2P6$ splits via period-doubling into three-cluster states $C3P12$ with partition $\{p_i^{(3)}\}_{i=1}^3$ such that $p_1^{(3)} + p_2^{(3)} = p_1^{(2)}$ and $p_3^{(3)} = p_2^{(2)}$ (bifurcation curve CD in Fig. 4, transition II in Fig. 10). If the splitting of the coherent state has been symmetric, the two cluster state $C2P6$ splits via temporal period-doubling into four-cluster states $C4P12$ with partition $\{p_i^{(4)}\}_{i=1}^4$ such that $p_1^{(4)} + p_2^{(4)} = p_1^{(2)}$ and $p_3^{(4)} + p_4^{(4)} = p_2^{(2)}$ (bifurcation point C in Fig. 4, transition III in Fig. 10). The state $C4P12$ can then bifurcate within the cluster subspace via Hopf bifurcation (curve CD in Fig. 9a, transition VII in Fig. 10) or it can split via temporal period-doubling into five-cluster states $C5P24$ (transition VIII

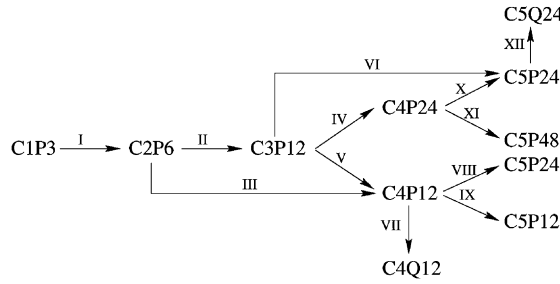


Fig. 10. Schematic representation of bifurcation sequences and emergence of clustered states that take place in system (1) after loss of stability by periodic coherent state. $CkPm$ denotes k -cluster states with period- m temporal dynamics (Q is for quasiperiodic motion).

in Fig. 10) with partition $\{p_i^{(5)}\}_{i=1}^5$ such that $p_1^{(5)} + p_2^{(5)} = p_1^{(4)}$ and $p_i^{(5)} = p_i^{(4)}$, $i = 2, 3, 4$ (bifurcation curve DE in Fig. 9a) or $p_i^{(5)} = p_i^{(4)}$, $i = 1, 2, 3$ and $p_4^{(5)} + p_5^{(5)} = p_4^{(4)}$ (bifurcation curve EF in Fig. 9a).

The three-cluster state $C3P12$ with partition $\{p_i^{(3)}\}_{i=1}^3$ loses its transverse stability either via transverse period-doubling or transcritical (pitchfork) bifurcation. In the latter case, the state $C3P12$ asymmetrically splits into four-cluster states $C4P12$ of the same temporal periodicity and with partition $\{p_i^{(4)}\}_{i=1}^4$ such that $p_1^{(4)} = p_1^{(3)}$, $p_2^{(4)} = p_2^{(3)}$, and $p_3^{(4)} + p_4^{(4)} = p_3^{(3)}$ (see Figs. 7 and 8, transition V in Fig. 10). The four-cluster state $C4P12$, in its turn, can bifurcate within the cluster subspace via Hopf bifurcation (curve CD in Fig. 7b, transition VII in Fig. 10) or split into five-cluster states via temporal period-doubling bifurcation (curve CD in Fig. 8, the $p_1^{(4)}$ -cluster splits, transition VIII in Fig. 10) or via transverse transcritical bifurcation (bifurcation curve AD in Fig. 8, the $p_4^{(4)}$ -cluster splits, transition IX in Fig. 10).

If the partition $\{p_i^{(3)}\}_{i=1}^3$ of the three-cluster state $C3P12$ admits period-doubling cluster splitting (see Section 5.1), then the clustered state $C3P12$ bifurcates either into four- or into five-cluster states. In the latter case which occurs when $p_1^{(3)} = p_2^{(3)}$, the state $C3P12$ splits into five-cluster states $C5P24$ with partition $\{p_i^{(5)}\}_{i=1}^5$ such that $p_1^{(5)} + p_2^{(5)} = p_1^{(3)}$, $p_3^{(5)} + p_4^{(5)} = p_2^{(3)}$, and $p_5^{(5)} = p_3^{(3)}$ (the bifurcation curve EF in Fig. 4 and the bifurcation point B in Fig. 6, transition VI in Fig. 10). The five-cluster state $C5P24$ can then bifurcate within its cluster subspace via Hopf or via period-doubling bifurcations (curves CD and EF, respectively, in Fig. 9b; transition XII in Fig. 10), or split into six-cluster states via temporal period-doubling (curves DE and FG in Fig. 9b; transition is not shown in Fig. 10).

In the case $p_1^{(3)} < p_2^{(3)}$, i.e., where the state $C3P12$ is born via asymmetric splitting of the two-cluster state $C2P6$, the cluster transition proceeds also through a temporal period-doubling. The state $C3P12$ splits into four-cluster states $C4P24$ (bifurcation curve AB in Fig. 6, the $p_1^{(3)}$ -cluster splits; transition IV in Fig. 10). With further decreasing the control parameter ε , the state $C4P24$ bifurcates into $C5P24$ -states via transcritical bifurcation (Fig. 6, the bifurcation curves BC and AF, where $p_3^{(4)}$ -cluster splits, and the bifurcation curves CD and EF, where $p_4^{(4)}$ -cluster splits; transition X in Fig. 10). The state $C4P24$ can also bifurcate into period-48 five-cluster states $C5P48$ (transition XI in Fig. 10) or six-cluster states $C6P48$ (bifurcation curve DE in Fig. 6, $p_1^{(4)}$ -cluster or both $p_1^{(4)}$ - and $p_2^{(4)}$ -clusters split via temporal period-doubling, respectively).

With regards to the transitions presented in Fig. 10, the bifurcations shown in Fig. 1 can be classified as follows:

- Fig. 1a: The transitions $I \rightarrow II \rightarrow V \rightarrow VIII$.
- Fig. 1b: The transitions $I \rightarrow III \rightarrow VII$.
- Fig. 1c: The transitions $I \rightarrow II \rightarrow IV \rightarrow X$.
- Fig. 1d: The transitions $I \rightarrow II \rightarrow VI \rightarrow XII$.

6. Conclusion

In this paper, we have described cluster-splitting bifurcations in globally coupled identical chaotic maps. We have focused on the simplest case, where the underlying dynamical regime is periodic. The main difficulty in the description of the cluster-splitting is in the enormous degeneracy of the linearized dynamics: If a cluster consisting of N_i elements becomes transversally unstable, $N_i - 1$ directions in the phase space become unstable simultaneously.

Our approach was to look for possible stable regimes that can result from the bifurcation in the simple classes of new-born solutions. In most cases stable supercritical regimes corresponding to splitting of unstable cluster in two new ones do exist. Nevertheless, a great amount of degeneracy still remains due to different possible partitions of elements between new-born clusters. We have demonstrated that in the case of period-doubling splitting only partitions with ratios between 1/2 and 2 are stable, although statistically seen more probable are partitions with ratios close to 1. This statistical feature of the cluster splitting requires the bifurcation diagram to be manifold: the later bifurcations depend essentially on the partitions in the previous ones. This multiplicity in bifurcation diagrams makes the population of coupled systems very complex even if the dynamics is not chaotic.

Acknowledgements

We thank E. Mosekilde for a number of illuminating discussions. O.P. thanks the Alexander-von-Humboldt Foundation for financial support. Yu.M. acknowledges support from DFG.

References

- [1] L. Brunnet, H. Chaté, P. Manneville, Long-range order with local chaos in lattices of diffusively coupled ODEs, *Physica D* 78 (1994) 141–154.
- [2] G. Osipov, A. Pikovsky, M. Rosenblum, J. Kurths, Phase synchronization effects in a lattice of non-identical Rössler oscillators, *Phys. Rev. E* 55 (1997) 2353–2361.
- [3] H. Bohr, K.S. Jensen, T. Petersen, B. Rathjen, E. Mosekilde, N.-H. Holstein-Rathlou, Parallel computer-simulation of nearest-neighbor interaction in a system of nephrons, *Parallel Comput.* 12 (1989) 113–120.
- [4] A. Pikovsky, M. Rosenblum, J. Kurths, Synchronization in a population of globally coupled chaotic oscillators, *Europhys. Lett.* 34 (1996) 165–170.
- [5] D. Zanette, A.S. Mikhailov, Condensation in globally coupled populations of chaotic dynamical systems, *Phys. Rev. E* 57 (1998) 276–281.
- [6] H. Chate, J. Losson, Non-trivial collective behavior in coupled map lattices: a transfer operator perspective, *Physica D* 103 (1997) 51–72.
- [7] T. Shibata, K. Kaneko, Collective chaos, *Phys. Rev. Lett.* 81 (1998) 4116–4119.
- [8] M. Cencini, M. Falcioni, D. Vergni, A. Vulpiani, Macroscopic chaos in globally coupled maps, *Physica D* 130 (1999) 58–72.
- [9] P. Grassberger, Synchronization of coupled systems with spatiotemporal chaos, *Phys. Rev. E* 59 (1999) R2520–R2522.
- [10] D. Topaj, W.-H. Kye, A. Pikovsky, Transition to coherence in populations of coupled chaotic oscillators: a linear response approach, *Phys. Rev. Lett.* 87 (2001) 074101.
- [11] W. Wang, I.Z. Kiss, J.L. Hudson, Experiments on arrays of globally coupled chaotic electrochemical oscillators: synchronization and clustering, *Chaos* 10 (2000) 248–256;
W. Wang, I.Z. Kiss, J.L. Hudson, Clustering of arrays of chaotic chemical oscillators by feedback and forcing, *Phys. Rev. Lett.* 86 (2001) 4954–4957.
- [12] K. Kaneko, Clustering, coding, switching, hierarchical ordering and control in network of chaotic elements, *Physica D* 41 (1990) 137–172;
K. Kaneko, Relevance of dynamic clustering to biological networks, *Physica D* 75 (1994) 55–73.
- [13] K. Kaneko, Coupled maps with growth and death: an approach to cell differentiation, *Physica D* 103 (1997) 505–527;
K. Kaneko, Dominance of Milnor attractors and noise-induced selection in a multiattractor system, *Phys. Rev. Lett.* 78 (1997) 2736–2739;
K. Kaneko, On the strength of attractors in a high-dimensional system: Milnor attractor network, robust global attraction, and noise-induced selection, *Physica D* 124 (1998) 322–344.
- [14] F. Xie, G. Hu, Clustering dynamics in globally coupled map lattices, *Phys. Rev. E* 56 (1997) 1567–1570;
F. Xie, H.A. Cerdeira, Clustering bifurcation and spatiotemporal intermittency in RF-driven Josephson junction series arrays, *Int. J. Bifurc. Chaos* 8 (1998) 1713–1718.

- [15] N.J. Balmforth, A. Jacobson, A. Provenzale, Synchronized family dynamics in globally coupled maps, *Chaos* 9 (1999) 738–754.
- [16] P. Glendinning, The stability boundary of synchronized states in globally coupled dynamical systems, *Phys. Lett. A* 259 (1999) 129–134; P. Glendinning, Transitivity and blowout bifurcations in a class of globally coupled maps, *Phys. Lett. A* 264 (1999) 303–310.
- [17] S.C. Manrubia, A.S. Mikhailov, Very long transients in globally coupled maps, *Europhys. Lett.* 50 (2000) 580–586; S.C. Manrubia, A.S. Mikhailov, Globally coupled logistic maps as dynamical glasses, *Europhys. Lett.* 53 (2001) 451–457.
- [18] A. Crisanti, M. Falcioni, A. Vulpiani, Broken ergodicity and glassy behavior in a deterministic chaotic map, *Phys. Rev. Lett.* 76 (1996) 612–615.
- [19] A.S. Pikovsky, J. Kurths, Collective behavior in ensembles of globally coupled maps, *Physica D* 76 (1994) 411–419.
- [20] N.F. Rulkov, Regularization of synchronized chaotic bursts, *Phys. Rev. Lett.* 86 (2001) 183–186.
- [21] M. Hasler, Yu. Maistrenko, O. Popovych, Simple example of partial synchronization of chaotic systems, *Phys. Rev. E* 58 (1998) 6843–6846; Yu. Maistrenko, O. Popovych, M. Hasler, On strong and weak chaotic partial synchronization, *Int. J. Bifurc. Chaos* 10 (2000) 179–203.
- [22] V.K. Vanag, L. Yang, M. Dolnik, A.M. Zhabotinsky, I.R. Epstein, Oscillatory cluster patterns in a homogeneous chemical systems with global feedback, *Nature (London)* 406 (2000) 389–391.
- [23] K. Miyakawa, K. Yamada, Synchronization and clustering in globally coupled salt-water oscillators, *Physica D* 151 (2001) 217–227.
- [24] M. Pollmann, M. Bertram, H. Hinrich Rotermund, Influence of time delayed global feedback on pattern formation in oscillatory CO oxidation on Pt(1 1 0), *Chem. Phys. Lett.* 346 (2001) 123–128.
- [25] O. Popovych, Yu. Maistrenko, E. Mosekilde, Loss of coherence in a system of globally coupled maps, *Phys. Rev. E* 64 (2001) 026205.
- [26] A. Pikovsky, O. Popovych, Yu. Maistrenko, Resolving clusters in chaotic ensembles of globally coupled identical oscillators, *Phys. Rev. Lett.* 87 (2001) 044102.
- [27] R.E. Amritkar, P.M. Gade, Wavelength doubling bifurcations in coupled map lattices, *Phys. Rev. Lett.* 70 (1993) 3408–3411; P.M. Gade, R.E. Amritkar, Spatially periodic orbits in coupled-map lattices, *Phys. Rev. E* 47 (1993) 143–154.
- [28] A.L. Gelover-Santiago, R. Lima, G. Martinez-Mekler, Synchronization and cluster periodic solutions in globally coupled maps, *Phys. A* 283 (2000) 131–135.
- [29] T. Shimada, K. Kikuchi, Periodicity manifestations in the turbulent regime of the globally coupled map lattice, *Phys. Rev. E* 62 (2000) 3489–3503.
- [30] N. Chatterjee, N. Gupte, Analysis of spatiotemporally periodic behavior in lattices of coupled piecewise monotonic maps, *Phys. Rev. E* 63 (2001) 017202.
- [31] K. Kaneko, Information cascade with marginal stability in a network of chaotic elements, *Physica D* 77 (1994) 456–472.
- [32] P. Ashwin, J. Buescu, I. Stewart, From attractor to chaotic saddle: a tale of transverse instability, *Nonlinearity* 9 (1996) 703–737.
- [33] O. Popovych, Yu. Maistrenko, E. Mosekilde, A. Pikovsky, J. Kurths, Transcritical loss of synchronization in coupled chaotic systems, *Phys. Lett. A* 275 (2000) 401–406; O. Popovych, Yu. Maistrenko, E. Mosekilde, A. Pikovsky, J. Kurths, Transcritical riddling in a system of coupled maps, *Phys. Rev. E* 63 (2001) 036201.